THE INFLUENCE OF MORPHOLOGY ON THE MECHANICAL PROPERTIES OF CRYSTALLINE POLYMERS

E. H. ANDREWS

Department of Materials, Queen Mary College, London

ABSTRACT

Stress–strain curves and related mechanical parameters such as initial moduli, yield stress and fracture stresses have been measured for a variety of semi-crystalline polymers possessing a range of controlled morphologies. The investigations described embrace (i) a study of the low-temperature properties of *trans*-polychloroprene with 18% crystallinity and morphologies varying from spherulitic to row-nucleated ('shish-kebab'), (ii) a study of the properties of *cis*-polyisoprene with about 30% crystallinity and morphologies from spherulitic, through row-nucleated to fibrillar, tested both above and below T_g, and (iii) a study of the deformation of spherulitic polyethylenes with crystallinities from about 40% to 85% and after various doses of γ-radiation.

These studies taken together provide considerable insight into the respective roles of the crystalline and amorphous phases in determining high-strain mechanical properties. Simple but physically realistic two-phase models are proposed to explain many of the observations.

1. INTRODUCTION

During the last decade a considerable number of studies have been made of the mechanisms involved in the deformation of semi-crystalline polymers. These range from work on the deformation of single polymer crystals[1–3] to that on the deformation of spherulitic structures[4–6] and these investigations have provided a rich store of information concerning the crystallographic processes by which polymer structures deform.

In contrast, relatively little has been done directly to correlate morphology with mechanical properties, perhaps mainly because the complex morphologies of semi-crystalline polymers are difficult to alter in a controlled manner and equally difficult to characterise precisely.

Only rather general correlations between morphology and mechanical parameters (e.g., elastic moduli or yield stresses) have therefore emerged and critical tests of theoretical models have been markedly lacking.

This paper, which reviews work in this field carried out in the author's laboratory, is a contribution to the quantitative study of morphology–property relationships in semi-crystalline polymers. It addresses itself both to the problems of morphological control and characterisation and to the

interpretation of high-strain mechanical data (stress-strain and fracture parameters) in terms of the known morphological variables.

Three distinct investigations are reported, involving respectively a low crystallinity (18%) *trans*-polychloroprene, an intermediate crystallinity (30%) *cis*-polyisoprene and a range of intermediate-to-high crystallinity (40%–85%) polyethylenes. The investigations are not identical but, rather, complementary. In the case of polychloroprene, starting morphologies were produced by crystallization above T_g either in an unstrained condition (spherulitic) or from a strained melt (row-nucleated) and characterized by thin-film electron microscopy and x-ray diffraction. A further morphology was produced by deforming spherulites above T_g, before testing at $-180°C$.

In the work on polyisoprene a range of morphologies from spherulitic, through row-nucleated to fibrillar were produced by crystallizing from a melt held at various strains. Characterisation was again by thin-film electron microscopy. For comparison, purely amorphous material at different pre-strains was also tested. A feature of this work was the variation of the temperature of test from above to well below the glass transition of the amorphous phase. The behaviours of identical crystal morphologies could thus be compared in a rubber-like and a glassy matrix, and startling differences were observed.

Finally, irradiation cross-linking was used on polyethylene single crystals and on a range of bulk polyethylenes in an attempt to distinguish the contributions of crystalline and amorphous phases to the bulk mechanical behaviour. The deformation of irradiated single crystals was studied using electron microscopy and diffraction and the effects of irradiation on bulk material were evaluated in the light of this information.

Detailed accounts of these separate studies have been, or will be, published elsewhere. The present paper summarizes the results and concentrates upon their interpretation.

2. STRUCTURE-PROPERTY RELATIONS IN POLYCHLOROPRENE

2.1 General and experimental details

The material used was a vulcanised 84% *trans*-polychloroprene (Neoprene W) which has a maximum crystallinity of some 18%. The morphology thus consists of well-differentiated crystalline and amorphous phases with the latter predominating and providing a matrix for the crystals. The more extensive investigation on *cis*-polyisoprene (see next section) had already shown that mechanical properties in an intermediate crystallinity polymer were most sensitive to morphological changes when the amorphous phase is glassy. All experiments on polychloroprene were thus carried out at $-180°C$, well below the glass transition of $-43°C$ of the vulcanizate.

Full details of the experiments are given in the paper by Andrews and Reeve[7] but, briefly, were as follows.

Morphology was studied in unvulcanized films cast from solution on to a water surface and sufficiently thin (*ca* 100 nm or less) for transmission electron microscopy. The films as cast are amorphous, and could therefore be allowed to crystallize either relaxed or after straining and at any desired temperature.

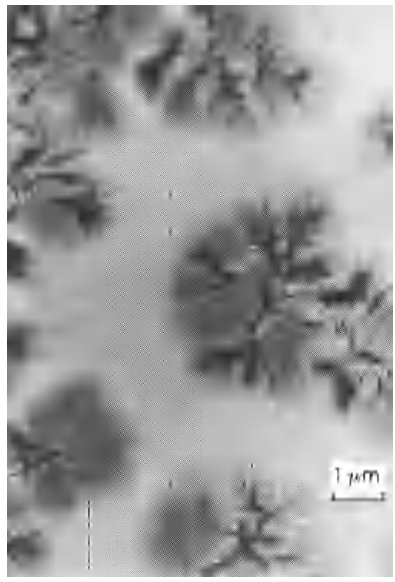

Figure 1. Partially crystallized thin film of polychloroprene (−5 °C, unstrained).

Crystallization could be halted at any time by staining with OsO_4 vapour[13] which also enhances contrast and stabilizes the specimen in the electron beam.

Figure 1 shows spherulites growing in an amorphous background and reveals their essentially lamellar constitution. When fully crystallized such films may be stretched whilst still floating on the water surface, and *Figure 2* shows the spherulites distorted to a strain of 200%, the lamellae retaining their identity in spite of the high plastic deformation. This deformation must be accommodated by a reasonably homogeneous plastic strain in the

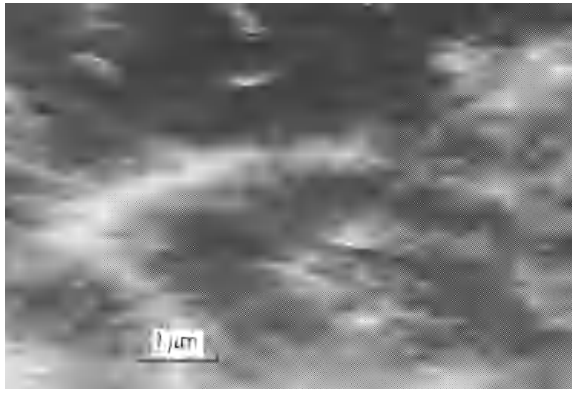

Figure 2. Distorted spherulites in a thin film of polychloroprene strained 200% at room temperature (Type II morphology)

lamellae themselves plus considerable molecular orientation in the inter-lamellar amorphous phase. Distorted spherulitic morphologies will be denoted Type II. Finally, films strained in their melt condition and allowed to crystallize produce the row-nucleated or 'shish-kebab' morphology shown (partially formed) in *Figure 3*. This morphology will be denoted Type I.

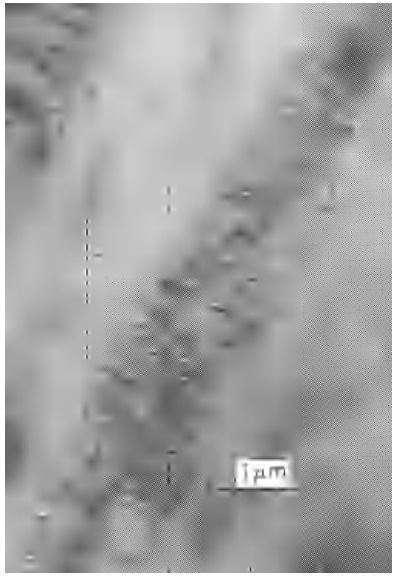

Figure 3. 'Shish-kebab' morphology in a partially crystallized film of polychloroprene held at 100% during crystallization at −5 C (Type I morphology)

It is clear that the same strain applied before crystallization (i.e. to the melt) and after crystallization, produces two quite different morphologies. Type I morphologies consist of 'shish-kebabs' with their 'backbones' highly oriented in the stretching direction and the lamellar crystals equally well oriented perpendicular to this direction. Type II morphologies contain distorted spherulites and relatively weak inter-spherulite boundaries which must carry any applied stress. The lamellae within the spherulites have a broad distribution of orientations but acquire a preferred orientation *in* the direction of extension as they deform in the amorphous matrix (see *Figure 2*). This might be expected to produce molecular axis alignment *perpendicular* to the stretching direction, since the molecules lie perpendicular to the lamellar surfaces. The x-ray data shows that this does not occur however at the high strains (> 100%) used here because the lamellae deform plastically by chain axis slip which tends to bring the molecules into the stretching direction and gives an overall molecular orientation *in* this direction.

Bulk specimens of the same polychloroprene were prepared by hot-pressing and were lightly vulcanised to prevent creep. Spherulitic morpholo-

gies were obtained directly by crystallizing at −5°C and Type II morphologies by straining spherulitic specimens at room temperature by various amounts. Amorphous reference specimens were prepared by straining specimens at room temperature by the desired amount, melting under strain *in vacuo* at 70°C for 2 h, and quenching rapidly to the testing temperature of −180°C. The same process produced Type I morphologies if, instead of quenching, the specimens were cooled to −5°C and held under strain for not less than 5 days. (Crystallization was taken to completion in all crystalline specimens.)

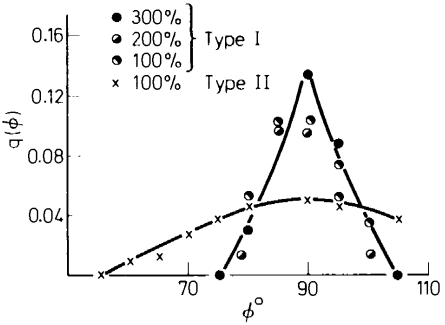

Figure 4. Plane normal distribution function $q(\phi)$ for the composite 200 + 120 reflection for different prestrains and morphologies

Wide angle x-ray measurements were used to characterize the bulk morphologies. The information obtained in this way is, of course, limited to the orientation of the unit cell and thus of the molecular axis, but this is sufficient to show whether bulk morphologies are consistent with thin film morphologies produced under the same conditions. The x-ray results (*Figure 4*) show that Type I morphologies achieve a very high *c* axis orientation at 100% melt strain and that this orientation is not significantly improved by higher melt strain. This is in excellent agreement with the thin-film micrographs of row-nucleated structures in which very precise alignment of lamellae perpendicular to the straining direction is observed at relatively low melt strain. In contrast to this, the *c* axis alignment in Type II morphologies is poor and increases progressively with applied strain in a way entirely consistent with the gradual distortion of pre-existing lamellar spherulites. It can safely be concluded that the general features of this film morphology are preserved in the vulcanized bulk.

As mentioned previously, stress–strain curves were taken for amorphous, Type I and Type II morphologies (for various prestrains) at a temperature of −180°C. It is important to note that the strains (100%, 200% and 300%) used to generate different morphologies were applied at room temperature and will be called prestrains, whereas testing was carried out below T_g at −180°C.

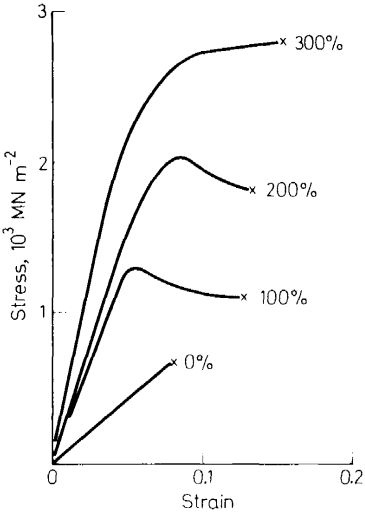

Figure 5. Nominal stress *vs* strain curves at −180 C for amorphous polychloroprene with various prestrains

2.2 Results and conclusions

Typical nominal stress *vs* strain curves for the oriented amorphous polymer are shown in *Figure 5*. For zero prestrain the behaviour is brittle (except at very low testing rates), but otherwise yield is observed followed by early fracture at strains of 12 to 15%. The effect of pre-orientation (always in the testing direction) is to raise the initial modulus and the yield stress by factors of up to five.

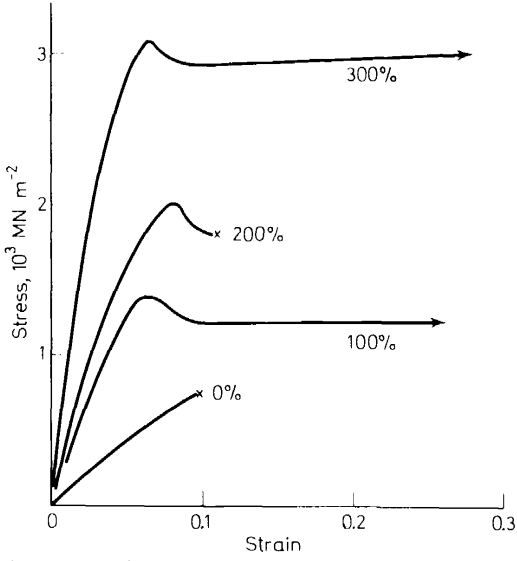

Figure 6. As *Figure 5* but for semi-crystalline material (Type I morphologies)

Specimens with Type I morphologies give nearly identical results to the amorphous materials except in respect of fracture strains (*Figure 6*). Initial moduli and yield stresses are similar to those for amorphous specimens with the same pre-orientations, but fracture strains frequently exceed 30%.

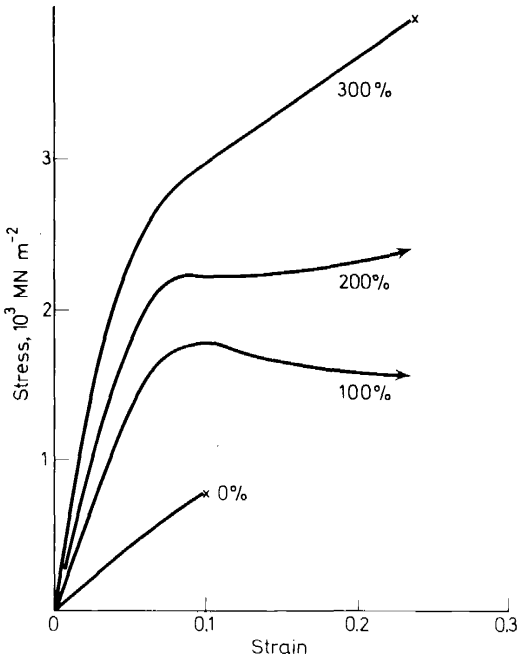

Figure 7. As *Figure 5* but for semi-crystalline material (Type II morphologies)

Post-yield deformation in these materials does not occur by necking, but by the propagation through the specimen of whitened bands of microvoiding[8]. The main effect of row-nucleated crystalline structures is thus not to modify the stiffness or yield behaviour of the amorphous phase, but simply to stabilize microvoiding and thus prevent premature fracture. This stabilization could be caused by the 'shish-kebabs' acting either as fibre reinforcement or as nuclei for cavitation under the hydrostatic component of the applied stress.

A minor point of interest is that Type I material at 300% pre-extension exhibits a 'yield drop' in stress whilst the corresponding amorphous specimens do not. Since yield drop occurs at all lower pre-extensions this suggests that the amorphous phase in Type I material is locally less oriented than the nominal 300%. This is to be expected as a result of crystallization under strain, the amorphous zones relaxing as the highly oriented crystalline regions develop, maintaining the average orientation at its nominal value.

The behaviour of Type II morphologies (*Figure 7*) is significantly different from that of amorphous and Type I structures. Whilst initial moduli are

similar, the yield stresses and strains are generally higher (by some 30% for 100% pre-extension reducing to no change for 300% pre-extension) and strain hardening is observed for the first time in the immediate post-yield region. This is indicated not only by the obvious rise of the 300% pre-strain curve in *Figure 7* but also by the more gradual yield drop at lower pre-extensions.

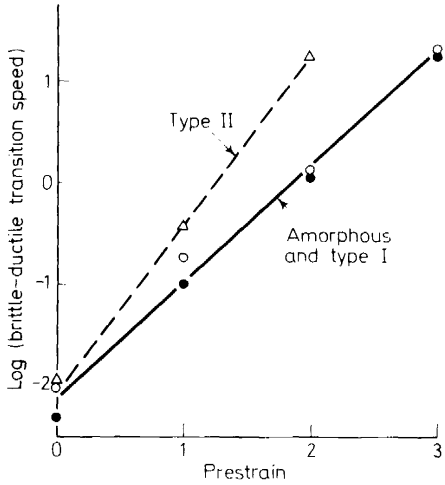

Figure 8. Brittle–ductile transition speed as a function of pre-orientation for different morphologies

By testing at different rates of strain, a brittle–ductile transition can be observed in these materials. That is, each kind of specimen is ductile (yields) at some rate of strain but brittle at a higher rate. The dependence of the brittle–ductile transition rate upon pre-extension is shown in *Figure 8*. Again, amorphous and Type I materials behave identically, though with a strong dependence on prestrain. Type II morphologies are markedly less brittle at equivalent pre-extensions, behaving as if the true amorphous orientation were some 50% higher than the nominal or pre-extension strain.

Both the stress–strain and brittle–ductile transition data indicate that the presence of low degrees of crystallinity has a negligible effect on mechanical properties compared with the molecular orientation in the amorphous phase. If, however, as in Type II morphologies, the presence of crystallinity is instrumental in modifying the state of orientation of the amorphous phase, quite large effects can be observed. The Type II brittle–ductile transition data can be interpreted very simply by saying that the average local amorphous orientation is enhanced by 50% due to the presence of crystalline material during prestraining. This is not the whole story, however, since Type II material is not significantly stiffer than the others, whereas increased amorphous orientation greatly enhances stiffness (see *Figure 5*). The answer to this paradox lies probably in the difference between local and average amorphous orientations. The complex nature of Type II morphologies

probably results in very high local amorphous alignments (as lamellae shear relative to one another) without a high average orientation, the local regions having poor mutual alignment. The bulk stiffness must depend on average orientation, but a locally initiated event like brittle fracture can be strongly inhibited by the local molecular organisation.

Post yield deformation by microvoid formation can also be modified by local amorphous alignment since the tensile stress necessary to promote void growth in an elastic–plastic solid is of the form[9]

$$\sigma = 2Y\left\{1 + \ln\frac{E}{3(1-\nu)Y}\right\}$$

where Y and E are the local yield stress and Young's modulus respectively. The high local yield stress of the highly oriented amorphous zones (see *Figure 5*), added to the finite extensibility of the amorphous network, are thus quite sufficient to explain the strain hardening observed in Type II morphologies.

3. STRUCTURE-PROPERTY RELATIONS IN *cis*-POLYISOPRENE

3.1 General and experimental

The second investigation to be described was far more extensive than the first and full details are available in the work of Reed[10]. As in the polychloroprene studies the morphologies obtained by crystallizing under varying degrees of melt strain were assessed using thin-film electron microscopy[11–14]. Spherulitic and row-nucleated structures were observed as for polychloroprene and at pre-extensions above 300% a new morphology, consisting essentially of row nuclei (or γ-filaments) without lamellar overgrowths, formed spontaneously at room temperature. By crystallizing natural rubber at melt strains from 0 to 750%, therefore, a whole sequence of morphologies could be grown (*Figure 9*). The effect of chemical crosslinking

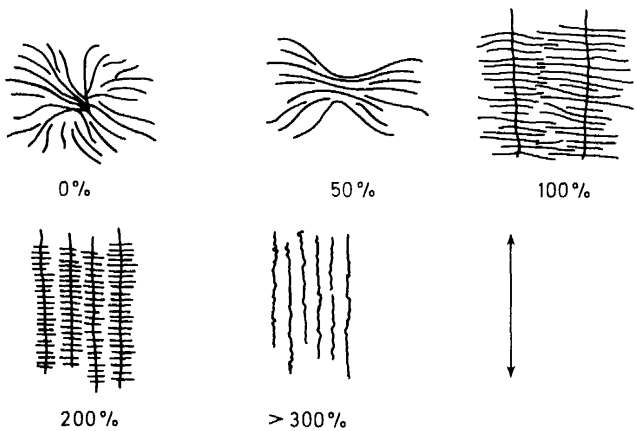

Figure 9. Morphologies developed in *cis*-polyisoprene at different melt strains (schematic). Strain axis vertical

was also assessed using thin films. The major effect was a sharp reduction in the length of row-nuclei, but the essential morphological features were otherwise unchanged.

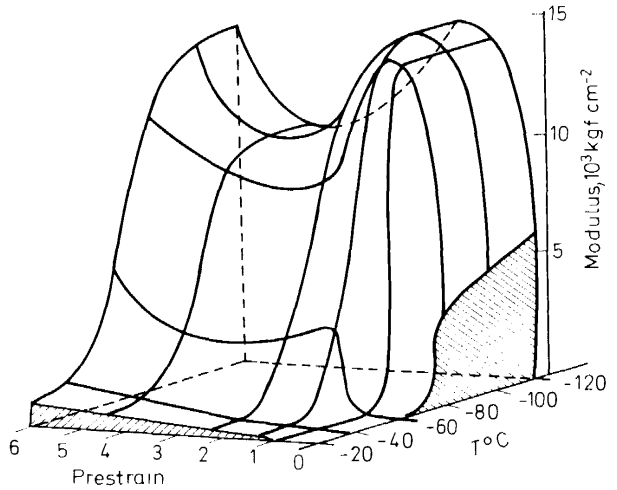

Figure 10a. Initial modulus for crystalline natural rubber as a function of prestrain (morphology) and testing temperature

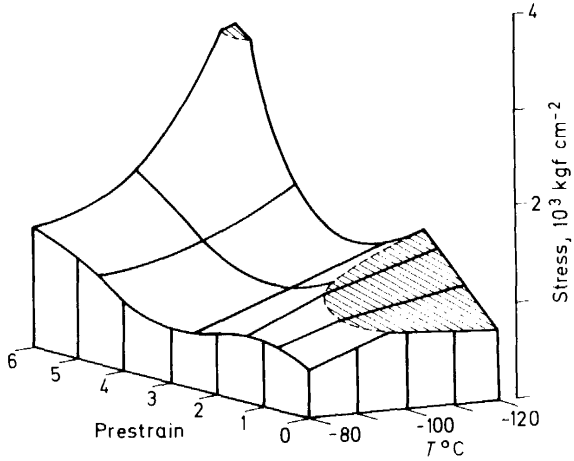

Figure 10b. As *Figure 10a* but for yield or brittle fracture (shaded) stresses

Mechanical testing was carried out (in the direction of prestrain) on all morphologies over a wide temperature range, from the crystallizing temperature of -26°C downwards, through the glass transition at -73°C, to -120°C. Mechanical parameters such as initial modulus, yield or brittle fracture strain were measured and displayed as 3-dimensional graphs. Those selected for discussion here are the data for initial modulus and yield (or brittle) stress (*Figures 10a* and *b*). In the 3-dimensional graphs, the

parameter of interest is plotted vertically and the horizontal axes are pre-extension (i.e. the melt strain under which crystallization occurred) and the temperature of testing. All crystallization was carried out at $-26°C$ and taken to completion, achieving a maximum value of 27% to 33% depending on the prestrain. The pre-extension axis represents the morphological variable, 0% corresponding to spherulitic textures, 0 to 100% to directional sheaf-like structures, 100 to 300% to an increasing population of row nucleated structures, and 300 to 750% to fibrillar textures.

3.2 Results and interpretation

(i) *Initial moduli* (*Figure 10a*)

The moduli above T_g for all morphologies are low (rubber-like) although the expected increase is found with pre-orientation due to increasing alignment of the amorphous matrix. Spherulitic material undergoes a sharp modulus increase as the temperature falls through the glass transition at $-73°C$, the vitrification of the amorphous phase being the obvious cause. For pre-extensions of 100% or more, as row-nucleation begins to dominate the morphology, the rise in modulus across T_g becomes suddenly diffuse, occurring over the wide temperature range $-40°C$ to $-80°C$. This coincides with the achievement of a highly ordered 'shish-kebab' morphology in which the lamellae are precisely aligned perpendicular to the stretching direction. The sudden stiffening at intermediate temperatures (e.g. $-60°C$) can be attributed to a 'fibre reinforcement' mechanism, the 'shish-kebabs' acting as discontinuous stiff fibres. At higher temperatures the amorphous material between 'shish-kebabs' (or more exactly the pliable lamella-amorphous sandwich regions surrounding the stiffer backbones) has too high a shear compliance to facilitate stress transfer from fibre to fibre and no reinforcement is developed. Likewise, well below T_g, the fibres are no longer significantly stiffer than the glassy matrix and do not produce reinforcement. The stiffening at 100% pre-extension is therefore significant only at intermediate temperatures, producing the gradual rise of modulus with temperature which is so noticeable in *Figure 10a*.

Below T_g the behaviour is complex. In low-crystallinity polychloroprene we found a five-fold increase in modulus, as pre-extension increased from zero to 300%, due entirely to amorphous orientation. Here at $-120°C$, as pre-extension rises from 0%, a comparable steep increase in modulus is observed due presumably to the same cause. This rise, however, continues only up to pre-extensions of 100% at which point the modulus begins to decrease to a saddle point at 400% pre-extension before rising again. This behaviour is almost certainly due to the establishment of relatively large amounts of 'shish-kebab' material at 100% pre-extension. The 'shish-kebab' lamellae have such good mutual alignment that they are able to deform *cooperatively* by crystallographic processes subject only to the restraint of the amorphous phase. The glassy matrix, furthermore, is almost totally broken up (in the direction of test) into a sandwich structure by the lamellar layers, so that its continuity and restraining power is minimized. These two effects occurring around 100% pre-extension combine to produce the sudden and surprising down-turn in modulus observed. As pre-extension increases further, the extent of the lamellar sheets decreases as row-nucleation density

rises and eventually a fibrillar morphology results with little or no lamellar crystallinity. The amorphous phase again becomes a continuous matrix and the low-temperature modulus resumes its rise with increasing pre-extension.

(ii) *Yield and brittle fracture* (*Figure 10b*)

Definite yielding and brittle fracture were only observed below T_g. At $-120°C$ the behaviour is qualitatively similar to polychloroprene at $-180°C$, showing a strong rise in yield stress with pre-extension, and brittleness at low pre-extension. As with modulus, however, there appears to be a temporary reduction in yield stress with increasing pre-extension after an initial rise and this can be explained in the same way as the modulus variations. That is, the formation of 'shish-kebabs' at pre-extensions exceeding 100% breaks up the glassy matrix into a sandwich structure allowing the crystalline phase a dominant role in deformation with the minimum restraint from the glassy matrix. The crystalline yield stress is potentially low because crystallographic yield mechanisms are available. Hence the rise in yield stress with amorphous alignment which dominates in polychloroprene at 18% crystallinity, is strongly offset by the lamellae at a crystallinity of 30%.

It is notable from *Figure 10b* that the steep rise of yield stress with pre-orientation only develops at low temperatures. Consequently the yield stress rises rapidly with falling temperature for highly oriented material but slowly for low and intermediate pre-extensions. Results (not shown) for oriented amorphous material exhibit a less sharp rise. If yield in the amorphous phase is regarded as an activated flow phenomenon, this can be thought to signify either that the activation energy for flow is higher for more highly oriented glasses or that the activation volume for flow is smaller (or both). The latter is perhaps the more interesting possibility, suggesting that smaller segments of the molecule are involved in the flow of highly oriented glasses than in isotropic material.

4. DEFORMATION OF IRRADIATED POLYETHYLENE

The basic idea behind the third investigation described in this paper[15] was to suppress crystallographic deformation processes by irradiation cross-linking and study the effects on bulk deformation behaviour. Here we are concerned with a range of crystallinities from 44% to 85%. We have already noted the increasing influence of crystallinity in passing from 18% (for polychloroprene) to 30% (for natural rubber), and it is to be expected that this trend will continue as the crystallinity continues to rise. The investigation was in two parts. Firstly, the effects of γ-irradiation on crystallographic deformation processes were monitored using single crystals of polyethylene deformed on an extensible substrate and viewed in the electron microscope. Secondly, tensile specimens, subjected to the same range of irradiation doses, were tested at room temperature. These specimens included polyethylenes of five different densities.

4.1 Deformation of irradiated single crystals

Full details of this work can be found elsewhere[16] and only the results will be summarized here. Unirradiated lamellar crystals deform by a variety of

crystallographic processes including chain-axis slip, other forms of slip, twinning and a phase change. Dislocations are active in some of these processes. Irradiation cross-linking was found to eliminate chain-axis slip, to strongly inhibit other slip systems and to suppress the phase change. It did not, however, prevent {110} twinning because only very small molecular displacements are necessary for this to take place. Moiré images revealed that cross-linking severely distorts the crystal lattice, the defect stress fields being long range, and this explains the strong inhibition of slip. Irradiated crystals moreover underwent micro-fracture on {100} and {010} planes (*Figure 11*) when deformed.

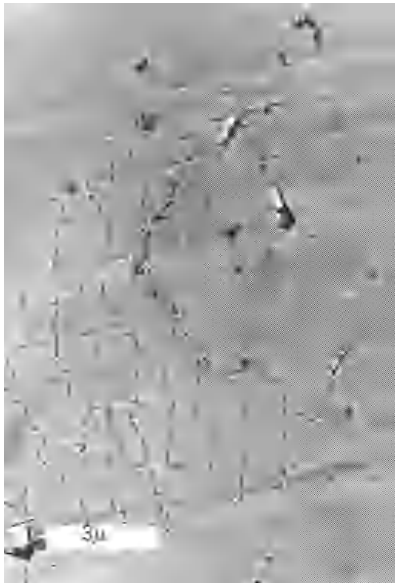

Figure 11. Deformed single crystal of irradiated polyethylene showing microfractures

Considered in terms of bulk behaviour, these results can be interpreted as follows. Increasing irradiation dose should initially produce a rapid increase in yield stress together, possibly, with post-yield strain hardening. Plastic strain at fracture will, however, decrease rapidly with dose. As the dose rises to 40 Mrad or more the crystals suffer internal or micro-fracture rather than gross fracture and thus continue to deform as intact entities but under decreasing stress. The question remains, how far these irradiation induced changes in the crystalline phase affect the deformation of bulk polyethylene, and how far they enable us to distinguish the separate roles of the crystalline and amorphous phases in such deformation. The effect of irradiation crosslinking on the amorphous phase itself is, in principle, known from experience with network elastomers.

4.2 Deformation of bulk polyethylene

Stress–strain data were obtained at 20°C and the regions prior to neck formation were converted to true stress *vs* strain curves. Typical data for unirradiated material is shown in *Figure 12* and for specimens exposed to a dose of 160 Mrad (*in vacuo*) in *Figure 13*. Three regions can be identified in these curves and are illustrated schematically in *Figure 14*. Region I (up to stress Y_1) is the initial, fairly linear, low compliance region; region II (up to stress Y_2) is a high compliance, post-yield region and region III (up to the necking stress Y_3) exhibits increasing strain hardening. At doses above 40 Mrad fracture occurs prior to Y_3 in all but the highest crystallinity material, whilst at 40 Mrad the two lowest crystallinity materials break before Y_3. For simplicity the slopes of the three regions in *Figure 14* will be denoted S_1, S_2 and S_3 respectively.

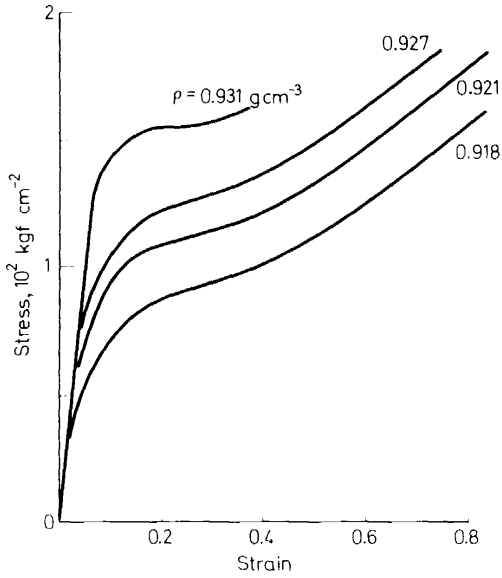

Figure 12. True stress *vs* strain curves at 20°C for some unirradiated polyethylenes up to neck formation

The initial slope S_1 is an increasing function of crystallinity but is virtually unaffected by radiation dose (*Figure 15*). Considering the drastic changes in crystallographic deformation processes observed in the single crystal work, one must conclude that S_1 owes little or nothing to plastic deformation of the crystalline phase since otherwise it would display some sensitivity to irradiation. The yield stress Y_1 is quite different in that it increases linearly with dose for the more crystalline specimens (*Figure 16*). The down-turn at 210 Mrad may be due to degradation of the polymer. Lower crystallinities show Y_1 almost constant with dose. Finally S_2 has a complex dependence upon dose, tending to rise in low crystallinity material but falling drastically to negative values in highly crystalline specimens (*Figure 17*). Many other

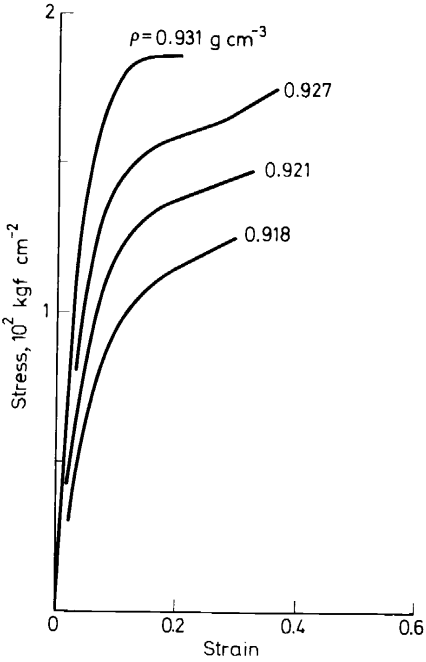

Figure 13. As *Figure 12* but for materials irradiated by 160 Mrad up to fracture

data could be presented. but discussion in this paper will be limited to those presented above.

Some of these results can be explained in fairly simple terms using a 'sandwich model' of crystal lamellae and amorphous zones (*Figures 18*) to picture the basic morphological unit undergoing deformation. Such units are, of course, randomly oriented in isotropic spherulitic polymers such as used here. In the 'unit' the lamellae are considered to undulate and come into contact randomly as shown; the probability of contact, and thus the average area of contact in a specimen, can be estimated in the following way.

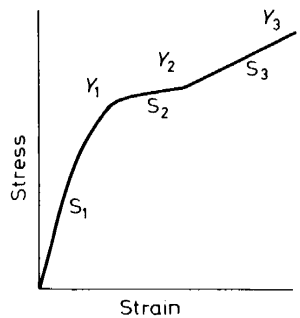

Figure 14. Schematic true stress *vs* strain curve for polyethylene

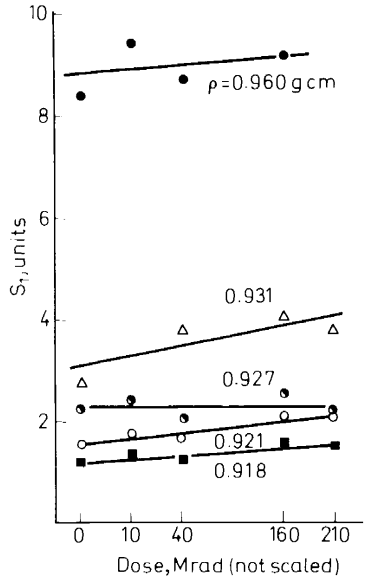

Figure 15. Effect of irradiation on initial slope S_1

Consider a cylindrical element of volume through the unit, its axis perpendicular to the (local) lamellar planes, as shown. Consider the element divided along its length into segments equal to the lamellar thickness l, which segments can be occupied by either a lamella or by amorphous material. (The implied quantization of amorphous phase into layers of thickness l can be avoided by a more complicated argument which, however, gives the same result.) The probability of any one segment containing a

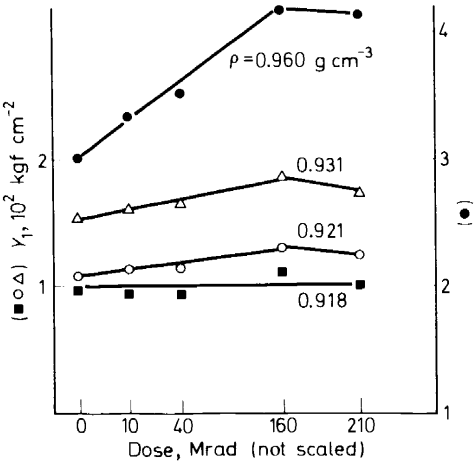

Figure 16. Effect of irradiation on yield stress Y_1

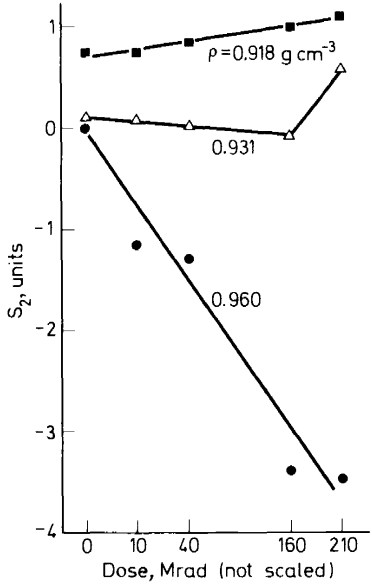

Figure 17. Effect of irradiation on slope S_2

lamella rather than amorphous material is simply L, the fractional volume of lamellar material. The probability of placing a second lamella in an adjacent segment is also L, so that the probability of two adjacent segments being occupied by crystalline material is L^2. If we consider adjacent segments to be in mechanical contact (e.g. linked by tie molecules), the probability of any element of lamellar surface being in such contact is thus L^2.

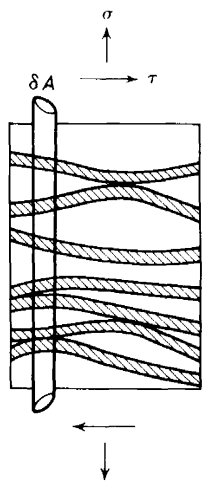

Figure 18. Morphological unit showing lamellae (shaded) in crystalline/amorphous sandwich structure. Note contact areas

Summing over a large area of lamellar surface, the area of contact will be L^2A where A is the total lamellar surface area.

Before making use of this result, values for L must be obtained. It might be thought that L could be equated to the crystallinity C, but this ignores the fact that up to 20% of amorphous material can be accounted for by the amorphous fold surfaces which, in one sense, are part of the lamellae. To compensate for this effect we shall allow the 'lamellarity' L to exceed the crystallinity C by 10%, i.e. the mean of 0 and 20%, since lamellae whose outer folds just touch may be considered as not in mechanical contact. Clearly any figure between about 5% and 15% could equally well be chosen.

$$L \simeq C + 0.1$$

Consider first the yield stress Y_1. If this point represents the breakdown of areas of mechanical attachment between lamellar surfaces (either by normal or shear stress according to the orientation of the units in the spherulite), we would expect Y_1 to be proportional to this area, i.e. to L^2.

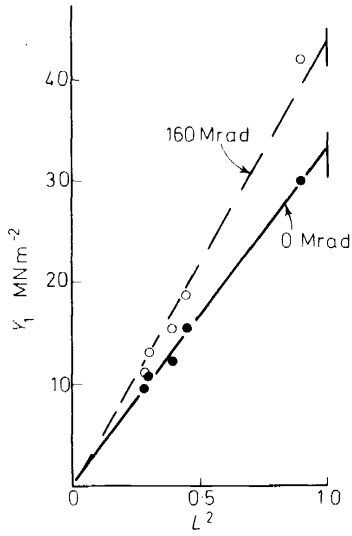

Figure 19. Effect of interlamellar adhesion on Y_1 for zero and 160 Mrad irradiation doses. Lines are theory, points are experimental

This is borne out remarkably as *Figure 19* shows. Both the data for un-irradiated and for 160 Mrad material plot linearly against L^2, the latter extrapolating to a much higher Y_1 value at $L = 1$. This extrapolated value is, of course, the actual yield stress for the attachment areas and since failure of these attachments probably occurs by yield in the adjacent regions of the lamellae themselves, $Y_1(L = 1)$ can be interpreted as the actual average yield stress of the crystalline phase. The increase in this quantity with irradiation dose (a factor of some 1.3 between 0 and 160 Mrad) is wholly consistent with the anticipated 'solid solution' hardening produced by

crosslinks in the lamellae. The $Y_1(L = 1)$ value for unirradiated material is some 30 MN/m^2 which is about half the yield stress for polycrystalline copper and twice that for basal glide in magnesium. It appears that we have, indirectly, achieved for the first time an estimate for the yield stress of a polymer single crystal and of its enhancement by crosslink 'hardening'.

The yield process Y_1 is thus envisaged as the breakdown of inter-lamellar attachments. The subsequent deformation is naturally a more compliant one, hence the low slope S_2 in this region. In low crystallinity material the deformation beyond Y_1 is probably controlled largely by the rubber-like amorphous zones which are now free to deform for the first time. Because these rubber-like zones become increasingly crosslinked by irradiation an increase in S_2 with dose is expected, as observed. In high crystallinity material,

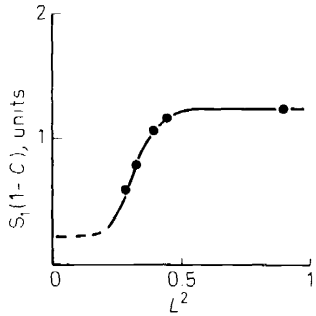

Figure 20. Corrected stiffness $S_1(1 - C)$ as a function of area fraction of attachments

however, the quantity of amorphous material (other than surface folds) reduces to nearly zero and S_2 must then be controlled by deformation of the lamellae. As the irradiation dose rises, however, the lamellae become increasingly liable to microfracture and will deform under decreasing stress as the fissures develop. A negative value for S_2 therefore agrees well with the single crystal data. The crack nucleation density in the lamellae will obviously govern the rate at which the lamellae lose their resistance to deformation and this density is known to increase about 2.5 times as the dose increases from 40 to 160 Mrad. This is very similar to the ratio of about 2.9 between S_2 for 160 Mrad and S_2 for 40 Mrad.

Finally, we consider the slope S_1. Its increase with increasing crystallinity is expected simply on the basis of the increasing amount of the crystalline phase (considered as 'hard' material at stresses below Y_1). The 'hard' material can be allowed for very simply by subtracting it from the deforming volume, so that the product

$$S_1(1 - C) = \text{constant}$$

If this product is plotted against C (or L^2, *Figure 20*) constancy is indeed observed for $L^2 > 0.4$ and implied for $L^2 < 0.1$. At intermediate crystallinities, however, the product rises rapidly indicating a morphological effect. This can be understood in terms of the unit model already discussed.

At low and high C the compliance of the composite can be regarded, respectively, as arising from the amorphous zones alone and the closely adjacent fold surface layers alone. At intermediate C, however, attachment areas are increasing in number and extent and a network of lamellae is being established which progressively takes over from the amorphous phase as the load bearing medium (see *Figure 21*). The increase in $S_1(1 - C)$ reflects this effect clearly. The lack of dependence of S_1 upon irradiation (*Figure 15*) also follows from this model since it nowhere involves plastic deformation of the crystalline phase.

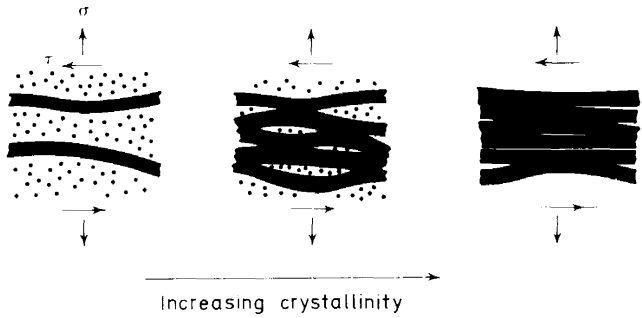

Figure 21. Morphological changes which affect the compliance as crystallinity increases. Lamellae black, amorphous dotted

5. CONCLUSION

In this paper a wide range of morphologies in low, intermediate and highly crystalline polymers have been discussed and the dependence upon them of certain mechanical properties established. Careful experimentation on the characterized morphologies, combined with the use of realistic two phase models allows the separate roles of crystalline and amorphous phases to be defined.

In view of the simplicity of the models employed, their success in explaining observations is highly encouraging.

6. ACKNOWLEDGEMENTS

As indicated by the references, this paper draws upon the work, some of it still unpublished, of several colleagues and research students. Particular acknowledgement is made to Dr. P. E. Reed and Dr. P. J. Owen for their work on natural rubber, to Mr. B. Reeve who studied polychloroprene and to Mrs. I. G. Voigt-Martin for the investigations on polyethylene.

REFERENCES

[1] P. H. Geil, *J. Polymer. Sci.* **A2**, 3813 (1964).
[2] H. Kiho, A. Peterlin and P. H. Geil, *J. Appl. Phys.*, **35**, 1599 (1964).
[3] H. Kiho, A. Peterlin and P. H. Geil, *J. Polymer Sci.* **B3**, 257 (1964).

[4] [a] V. B. Gupta, A. Keller and I. M. Ward, *J. Macromol. Sci.* **B2**, 139 (1968); [b] *J. Macromol. Sci.* **B4**, 453 (1970).
[5] I. L. Hay, and A. Keller, *Kolloid Z.Z. Polymere* **204**, 43 (1965).
[6] I. M. Ward (Ed.), *Orientation Phenomena in Polymers, J. Mater. Sci.* **6**, 451–582 (1971).
[7] E. H. Andrews and B. Reeve, *J. Mater. Sci.* **6**, 547 (1971).
[8] E. H. Andrews, *J. Polymer Sci.* **B5**, 317 (1967).
[9] R. Hill, *The Mathematical Theory of Plasticity*, p. 104. Oxford University Press (1950).
[10] P. E. Reed, *The Influence of Crystalline Texture on the Tensile Properties of Natural Rubber.* Ph.D. Thesis, University of London (1970).
[11] E. H. Andrews, *Proc. Roy. Soc.* **A270**, 232 (1962).
[12] E. H. Andrews, *Proc. Roy. Soc.* **A277**, 562 (1964).
[13] E. H. Andrews, P. J. Owen, and A. Singh, *Proc. Roy. Soc.* **A324**, 79 (1971).
[14] P.J. Owen, *Crystallization in Thin Films of Natural Rubber.* Ph.D. Thesis, University of London (1970).
[15] I. G. Martin, *Deformation of Irradiated Polyethylene Crystals.* Ph.D. Thesis, University of London (1969).
[16] E. H. Andrews and I. G. Voigt-Martin, *Proc. Roy. Soc.* **A327**, 251 (1972).